iScience, Volume *23*

Supplemental Information

Tricalbins Are Required for Non-vesicular Ceramide Transport at ER-Golgi Contacts and Modulate Lipid Droplet Biogenesis

Atsuko Ikeda, Philipp Schlarmann, Kazuo Kurokawa, Akihiko Nakano, Howard Riezman, and Kouichi Funato

SUPPLEMENTAL FIGURES

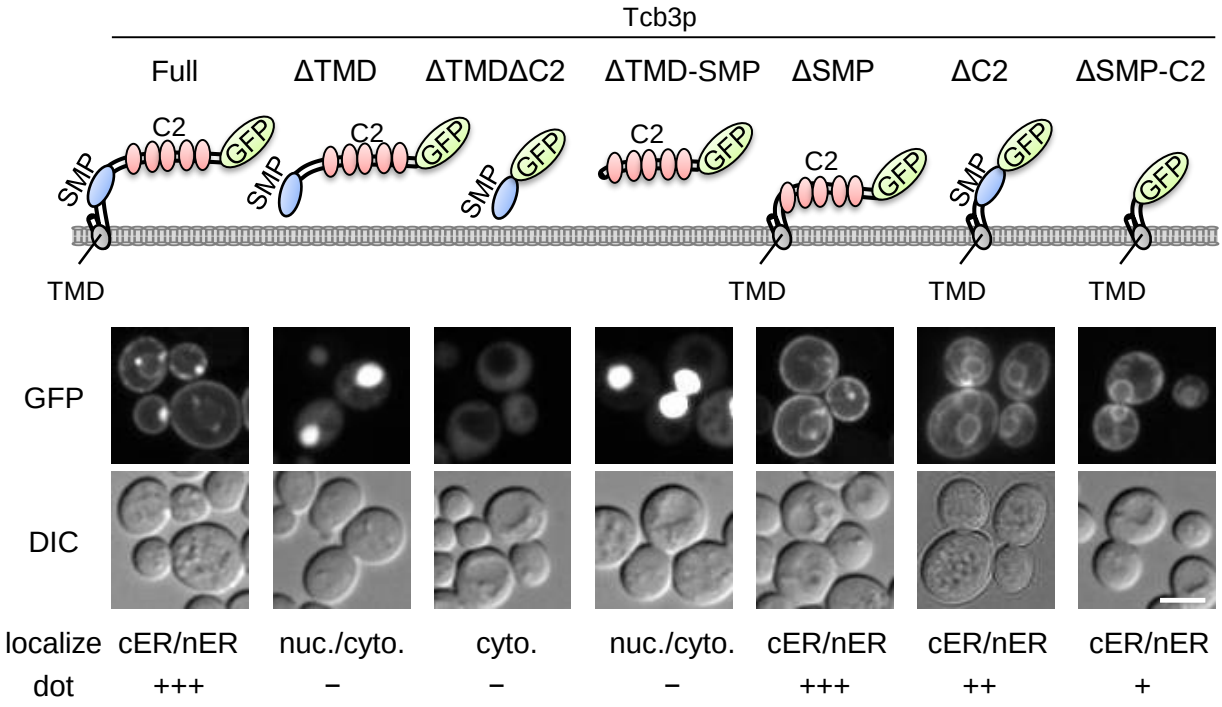

Figure S1. Truncated forms of Tcb3 lacking the transmembrane domain are distributed in the cytosol or nucleus, Related to Figure 1

*tcb3*Δ cells overexpressing Tcb3-GFP, Tcb3(ΔTMD)-GFP, Tcb3(ΔTMDΔC2)-GFP, Tcb3(ΔTMD-SMP)-GFP, Tcb3(ΔSMP)-GFP, Tcb3(ΔC2)-GFP or Tcb3(ΔSMP-C2)-GFP under *TDH3* promoter were grown at 25˚C and imaged by DIC and fluorescence microscopy. Scale bar, 5 μm.

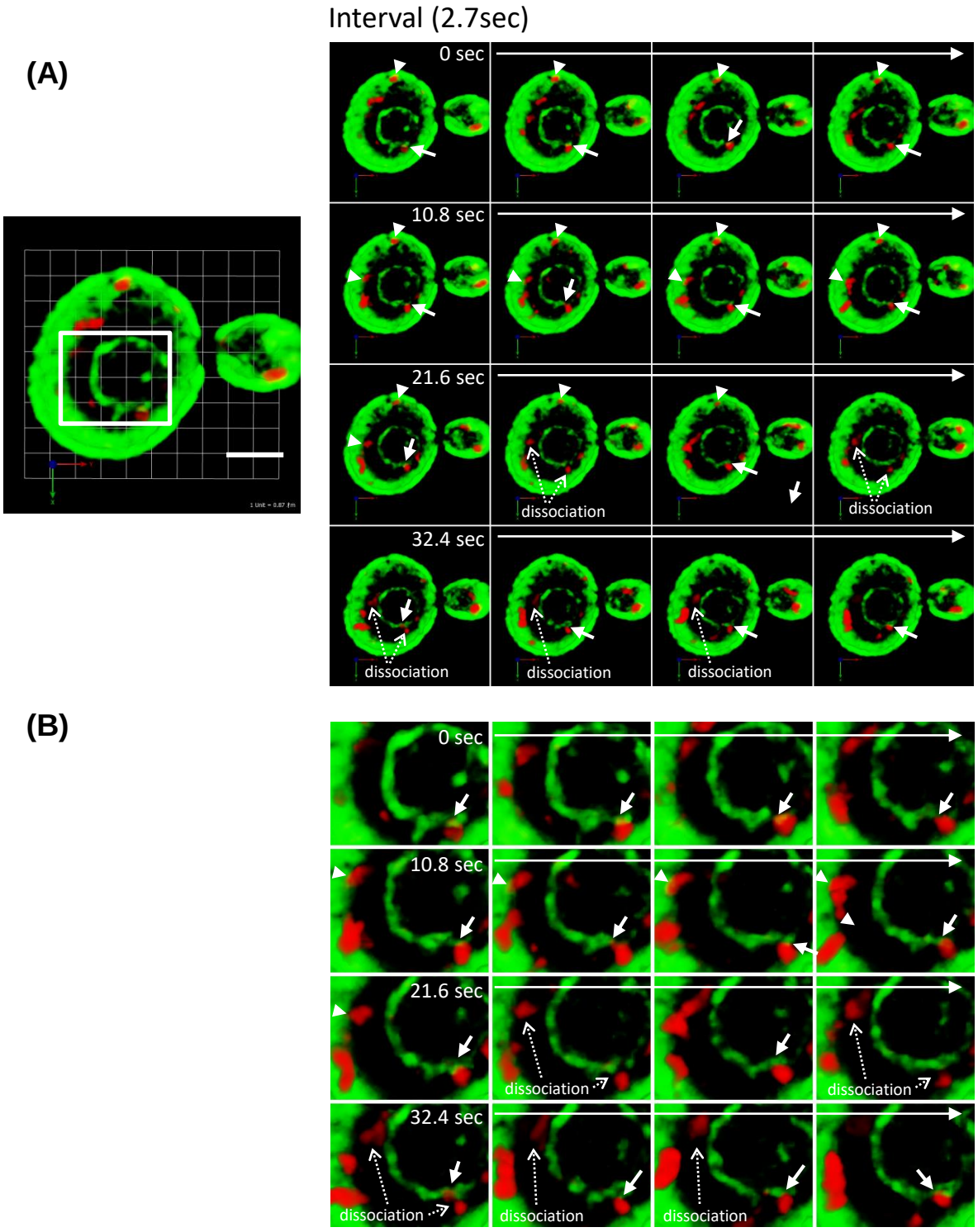

Figure S2. **Dynamic behaviors of ER-medial-Golgi contact sites, Related to Figure 2**

(A, B) *tcb3*Δ cells expressing Tcb3-GFP with mRFP-Gos1 under *TDH3* promoter were observed with SCLIM as in Fig 2B. Representative 3D images of a whole cell are shown. Right panels show time-lapse images (A). The boxed areas of the images in (A) are shown in an enlarged view (B). Scale bar, 2 μm. Arrows in the images indicate nER-medial-Golgi contact sites and arrowheads point to cER-medial-Golgi contact sites. The medial-Golgi contacts the nER or the cER (arrows and arrowheads) and then leave (dashed arrows).

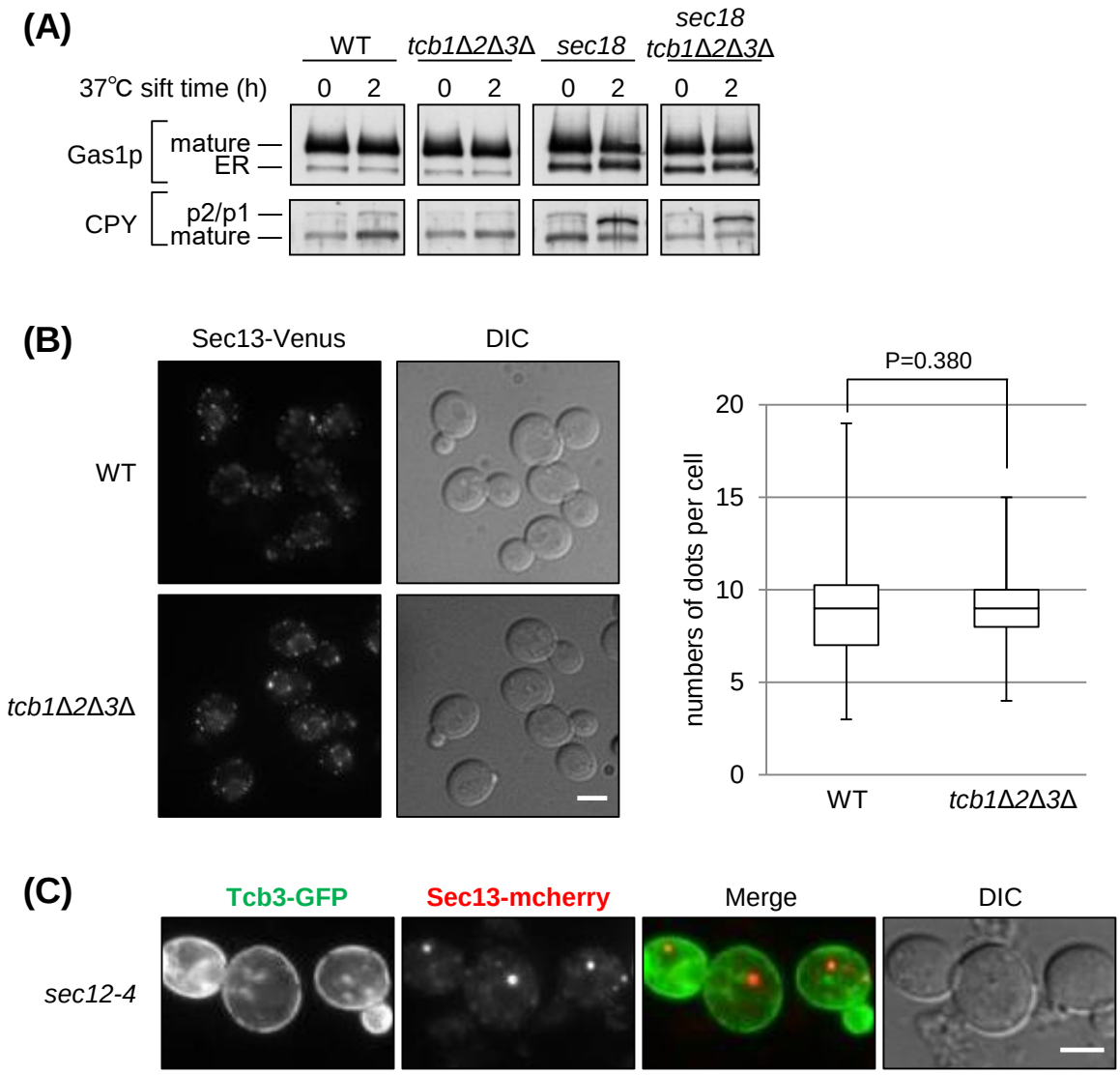

Figure S3. Tcb proteins are not required for ER-to-Golgi vesicular transport of proteins, Related to Figure 2 and Figure 4

(A) Cells were grown at 25˚C, shifted to 37˚C for 2 h. Cell lysates were prepared, subjected to SDS-PAGE, and analyzed by western blotting using antibodies against Gas1p and CPY. mature, mature forms of Gas1p and CPY; ER, immature ER form of Gas1p; p1 and p2, ER and Golgi forms of CPY, respectively.
(B) Cells expressing Sec13-Venus were grown at 25 ˚C and imaged by DIC and fluorescence microscopy. Scale bar, 5 μm. Numbers of dots per cell were counted. The box plot of the number of dots from more than 100 cells for each strain was shown. P value by Student's t-test.
(C) *sec12-4* cells expressing Tcb3-GFP and Sec13-mCherry were grown at 25˚C, sifted to 30˚C for 1 h, and imaged by DIC and fluorescence microscopy. Scale bar, 5 μm.

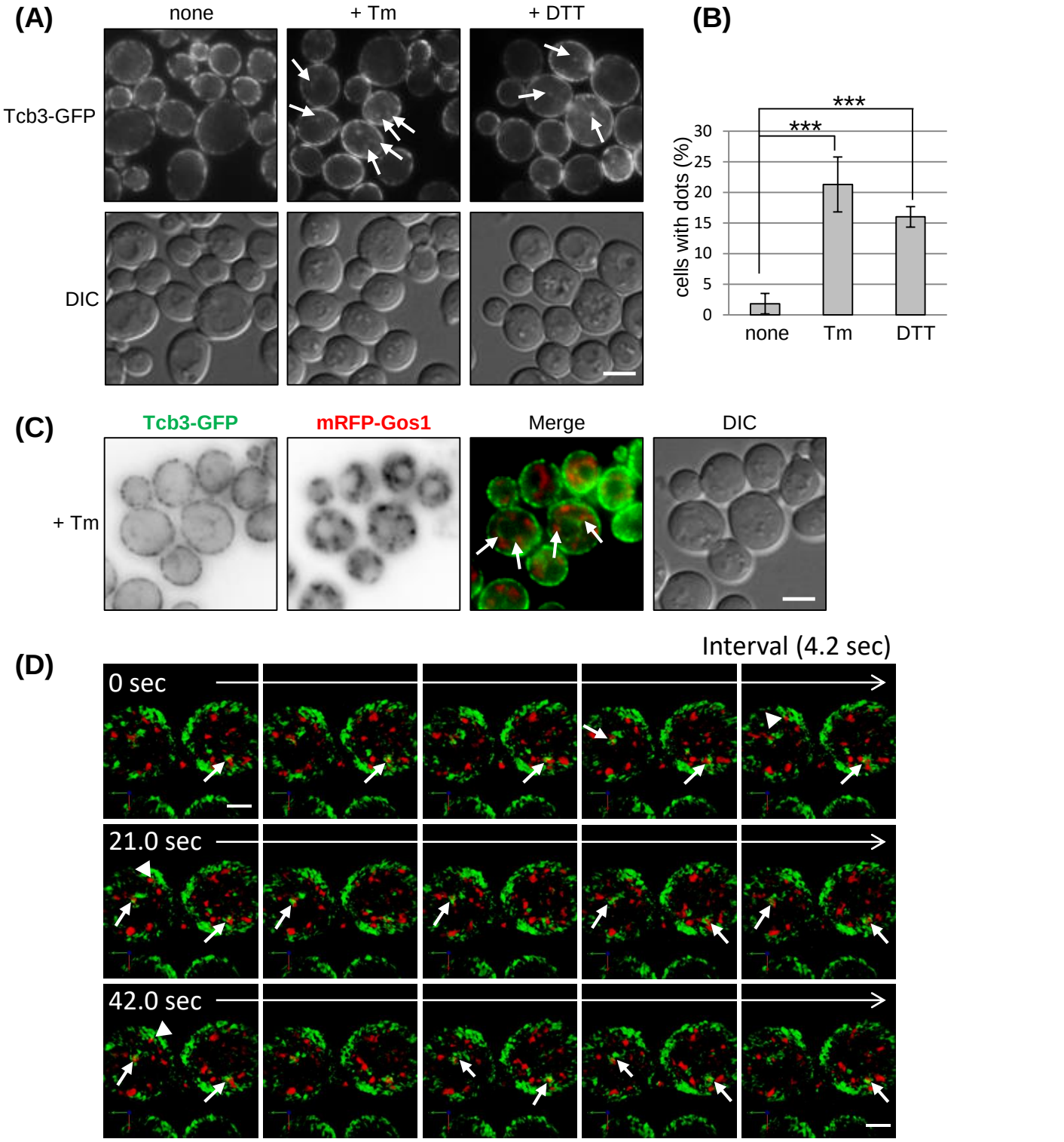

Figure S4. Tcb3p moves to nER-Golgi contact site in response to ER stress, Related to Discussion

(A, B) Cells expressing Tcb3p tagged with GFP at the C terminus under the control of *TCB3* endogenous promoter were grown at 25˚C, treated without and with tunicamycin (2.5 μg/ml, 4 h) or DTT (10 mM, 4 h), and imaged by differential interference contrast (DIC) and fluorescence microscopy. Arrows in the images indicate Tcb3-GFP dots (A). Scale bar, 5 μm. Percentages of cells with GFP dots were quantified, and the data represent the mean ± SD of three independent experiments; n > 300 cells. *** $P < 0.001$ by Student's t-test. (B).

(C, D) The same cells as in (A) were transformed with mRFP-*GOS1* plasmid, treated with tunicamycin (2.5 μg/ml, 4 h), and imaged by DIC and fluorescence microscopy (scale bar, 5 μm) (C). Cells were also observed with SCLIM (scale bar, 2 μm) (D). Arrows in the images indicate nER-medial-Golgi contact sites and arrowheads point to cER-medial-Golgi contact sites.

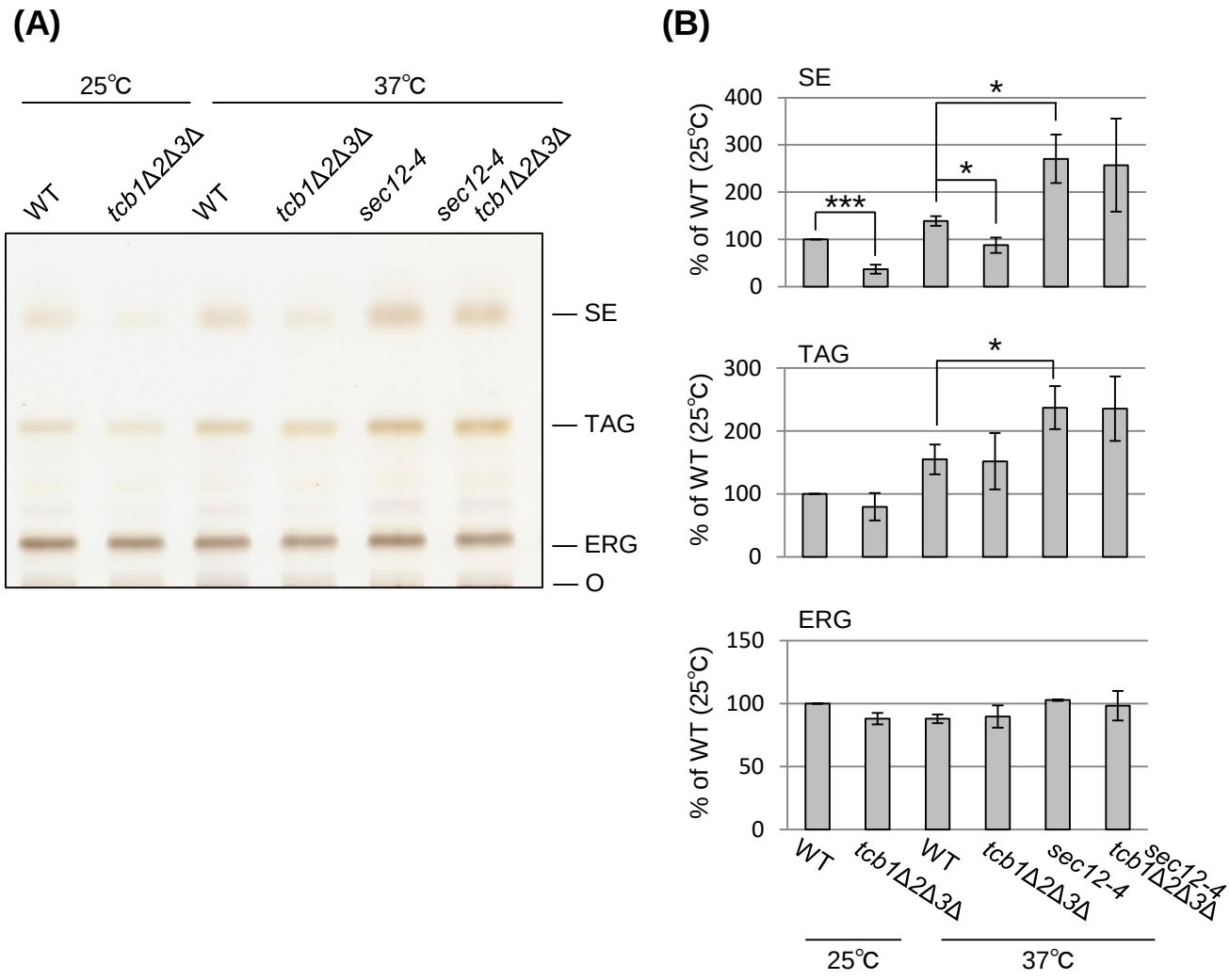

Figure S5. TLC analysis of the neutral lipids, Related to Discussion

Total lipids were extracted from wild-type and mutant cells grown at 25˚C or sifted to 37˚C for 30 minutes and separated on TLC plates (A). The positions of sterol ester (SE), triacylglycerol (TAG), ergosterol (ERG) and origin (O) are indicated. The bands were quantified with ImageJ and the relative levels of lipids to wild type cells grown at 25˚C were presented as percentage (B). Data represent mean ± SD of three independent experiments. *, $P < 0.05$; ***, $P < 0.001$ by Student's t-test.

SUPPLEMENTAL TABLES

Table S1. - Plasmids used in this study, Related to All Figures

Plasmid	Relevant information	Sorce
pRS416-*TDH3*/*TCB3*-GFP	*CEN,* yeast *TDH3* promoter, *TCB3-GFP*, *URA3*	This study
pRS416-*TDH3*/*TCB3*(ΔC2-SMP)-GFP	*CEN,* yeast *TDH3* promoter, $TCB3^{1F\text{-}259R}$*-GFP*, *URA3*	This study
pRS416-*TDH3*/*TCB3*(ΔSMP)-GFP	*CEN,* yeast *TDH3* promoter, $TCB3^{260F\text{-}488R\Delta}$*-GFP*, *URA3*	This study
pRS416-*TDH3*/*TCB3*(ΔC2)-GFP	*CEN,* yeast *TDH3* promoter, $TCB3^{1F\text{-}489R}$*-GFP*, *URA3*	This study
pRS416-*TDH3*/*TCB3*(ΔTMD)-GFP	*CEN,* yeast *TDH3* promoter, $TCB3^{260F\text{-}1546R}$*-GFP*, *URA3*	This study
pRS416-*TDH3*/*TCB3*(ΔTMD-SMP)-GFP	*CEN,* yeast *TDH3* promoter, $TCB3^{490F\text{-}1546R}$*-GFP*, *URA3*	This study
pRS416-*TDH3*/*TCB3*(ΔTMD ΔC2)-GFP	*CEN,* yeast *TDH3* promoter, $TCB3^{260F\text{-}489R}$*-GFP*, *URA3*	This study
pRS314-*TDH3*/ mRFP-*SED5*	*CEN*, yeast *TDH3* promoter, *mRFP-SED5*, *TRP1*	Provided by A. Nakano (Matsuura-Tokita et al., 2006)
pRS314-*TDH3*/ mRFP-*GOS1*	*CEN*, yeast *TDH3* promoter, *mRFP-GOS1*, *TRP1*	Provided by A. Nakano

		(Matsuura-Tokita et al., 2006)
YCplac22 / *SEC7*-mRFP	*CEN*, yeast *ADH1* promoter, *SEC7-mRFP*, *TRP1*	This study
pRS413-*ADH1* / *Kar2-SS-GFP-HDEL*	*CEN, yeast ADH1* promoter, *KAR2(1-135)-GFP-HDEL, HIS3*	This study
pRS416-*TDH3*	*CEN*, yeast *TDH3* promoter, *URA3*	Provided by M. Funk (Mumberg et al., 1995)
pRS413-*ADH1*	*CEN*, yeast *ADH1* promoter, *HIS3*	Provided by M. Funk (Mumberg et al., 1995)
pRS416-*TDH3* / *TCB3*	*CEN*, yeast *TDH3* promoter, *TCB3, URA3*	This study
pRS416-*TDH3* / *TCB3*(ΔC2-SMP)	*CEN,* yeast *TDH3* promoter, $TCB3^{1F\text{-}259R}$, *URA3*	This study
pRS416-*TDH3* / *TCB3*(ΔSMP)	*CEN,* yeast *TDH3* promoter, $TCB3^{260F\text{-}488R\Delta}$, *URA3*	This study
pRS416-*TDH3* / *TCB3*(ΔC2)	*CEN,* yeast *TDH3* promoter, $TCB3^{1F\text{-}489R}$, *URA3*	This study

Table S2 - Yeast strains used in this study, Related to All Figures

Strain	Genotype	Sorce
FKY66 / RH5574	MAT**alpha** *ura3 leu2 his3 trp1 bar1*	This study
FKY73 / RH5578	MAT**alpha** *ura3 leu2 his3 trp1 lys2 bar1 tcb1Δ::TRP1 tcb2Δ::HIS3 tcb3Δ::LEU2*	This study
FKY74 / RH5579	MAT**alpha** *ura3 leu2 his3 trp1 bar1 sec18-20*(ts)	This study
FKY76 / RH5584	MAT**alpha** *ura3 leu2 his3 trp1 lys2 bar1 sec18-20*(ts) *tcb1Δ::TRP1 tcb2Δ::HIS3 tcb3Δ::LEU2*	This study
FKY2924	MAT**a** *ura3 leu2 his3 trp1 lys2 bar1 tcb3Δ::LEU2*	This study
FKY2926	MAT**a** *ura3 leu2 his3 trp1 bar1 sec18-20*(ts) *tcb1Δ::TRP1 tcb2Δ::HIS3 tcb3Δ::LEU2*	This study
FKY2927	MAT**a** *ura3 leu2 his3 trp1 lys2 bar1 tcb1Δ::TRP1 tcb2Δ::HIS3 tcb3Δ::LEU2*	This study
FKY2928	MAT**alpha** *ura3 leu2 his3 trp1 lys2 bar1*	This study
FKY2929	MAT**alpha** *ura3 leu2 his3 trp1 bar1 sec18-20*(ts)	This study
FKY2960	MAT**a** *usa3 leu2 his3 lys2 bar1 sec12-4*(ts)	This study
FKY2984	MAT**alpha** *ura3 leu2 his3 trp1 lys2 bar1 sec12-4*(ts) *tcb1Δ::TRP1 tcb2Δ::HIS3 tcb3Δ::LEU2*	This study

FKY3343	MAT**a** *ura3 leu2 his3 trp1 lys2 bar1 TCB3-GFP::TRP1*	This study
FKY4663	MAT**a** *ura3 leu2 his3 trp1 lys2 bar1 SEC13-Venus::KanMX*	This study
FKY4876	MAT**a** *ura3 leu2 his3 trp1 lys2 bar1 tcb1Δ::TRP1 tcb2Δ::HIS3 tcb3Δ::LEU2 SEC13-Venus::KanMX*	This study
FKY4892	MAT **alpha** *ura3 leu2 his3 trp1 lys2 ade2 dga1Δ:: KanMX lro1Δ:: KanMX*	This study
FKY4987	MAT**a** *ura3 leu2 his3 lys2 bar1 sec12-4*(ts) *tcb3Δ::LEU2 SEC13-mCherry::KanMX*	This study
FKY5167	MAT **alpha** *ura3 leu2 his3 trp1 lys2 bar1 tcb1Δ::KanMX tcb2Δ::HIS3 tcb3Δ::LEU2*	This study

TRANSPARENT METHODS

Strains and Plasmids

All yeast plasmids and strains used in this study are listed in Table S1 and S2, respectively. Yeast cultivations, genetic manipulation and strain construction were carried out as described previously (Kajiwara et al., 2015, 2008). GFP-, Venus- and mCherry-tagged strains and *tcb* deletion strains were generated by PCR based one step gene replacement. Then, *tcb1*Δ*2*Δ*3*Δ strain was crossed with *sec18-20* or *sec12-4* strain to obtain the *sec tcb* combined double, triple and quadruple mutant strains. To construct the Tcb3-GFP, Tcb3(ΔSMP-C2)-GFP, Tcb3(ΔSMP)-GFP, Tcb3(ΔC2)-GFP and Tcb3p overexpression plasmids (*TCB3*, *TCB3*-ΔSMP, *TCB3*-ΔC2 and *TCB3*-ΔSMP-C2), appropriate regions of *TCB3* which were PCR amplified from yeast genomic DNA and GFP regions which obtained from pGREG600, were inserted into pRS416-*TDH3*. YCplac22/*SEC7*-mRFP plasmid was constructed from YCplac22 and pRS316-ADH/*SEC7*-Mrfp (Kurokawa et al., 2014). The BamHI-ClaI fragment containing Kar2p signal-peptide sequence (1-135) and the ClaI-XhoI fragment containing TAT2-mRFP were cloned into the BamHI-XhoI site of pRS413-ADH to generate pRS413-ADH/Kar2-SS-GFP-HDEL.

Fluorescence microscopy

Cells were grown overnight in SD medium including the appropriate nutrients to select for plasmids, and imaged by differential interference contrast (DIC) and fluorescence microscopy. GFP signals were measured by the Image J software. For parallel section observation, images were taken at z-sections with 0.2 μm parallel

intervals. For lipid droplet detection, cells were treated with Nile Red (final concentration to be 1μg/ml) for 10 minutes, and imaged by fluorescence microscopy. Fluorescence observation by super-resolution confocal live imaging microscopy (SCLIM) was performed as described previously (Kurokawa et al., 2014).

Lipid labelling

In vivo labelling of lipids with [^{3}H]*myo*-inositol (Perkin Elmer, Inc.) or [^{3}H]dihydrosphingosine (DHS; American Radiolabeled Chemicals Inc.) was performed as described previously (Kajiwara et al., 2008). Radiolabeled lipids were extracted with chloroform-methanol-water (10:10:3, vol/vol/vol), and analyzed by thin-layer chromatography (TLC) using solvent system I, chloroform-methanol-0.25% KCl (55:45:10, vol/vol/vol) for complex sphingolipid labeled with [^{3}H]*myo*-inositol and solvent system II, chloroform-methanol-4.2 N ammonium hydroxide (9:7:2, vol/vol/vol) for sphingolipid labeled with [^{3}H]DHS. For ceramide and acylceramide analysis, the lipids labelled with [^{3}H]DHS were first separated on TLC plates as above. Subsequently, fractions containing ceramides and actlceramides, which are approximately 2–3 cm from the top of the TLC plates (Kajiwara et al., 2012), were collected by scraping and eluting with chloroform-methanol (1:1, v/v), and analyzed by TLC using solvent system III, chloroform-methanol-2M ammonium hydroxide (40:10:1, vol/vol//vol) (Voynova et al., 2012). Radiolabeled sphingolipids were visualized and quantified on an FLA-7000 system.

Western blot analysis

Preparation of cell lysates and western blot analysis were performed as described

previously (Kajiwara et al., 2008). Blots were probed with rabbit polyclonal antibodies against Gas1p and CPY and a peroxidase-conjugated affinity-purified anti-rabbit IgG antibody.

Neutral lipid analysis

For the analysis of neutral lipids, cells corresponding to 10 OD_{600} were disrupted with glass beads, and lipids were extracted with chloroform-methanol-water (10:10:3, vol/vol/vol). The lipid extracts were applied to two step TLC as described before (Athenstaedt et al., 1999; Froissard et al., 2015); first step using petroleum-diethyl ether-acetic acid (25:25:1, vol/vol/vol) for the first third of the total distance and second step using petroleum-diethyl ether (49:1, vol/vol). To visualize the separated bands of neutral lipids, the TLC plates were dipped for 10 s into a developing solution (0.63 g of $MnCl_2 \cdot 4H_2O$, 60 ml of water, 60 ml of methanol, and 4 ml of concentrated sulfuric acid), briefly dried, and heated at 100°C for 30 min. Quantification of lipids was carried out using ImageJ.

SUPPLEMENTAL REFERENCES

Athenstaedt, K., Zweytick, D., Jandrositz, A., Kohlwein, S.D., and Daum, G. (1999) Identification and characterization of major lipid particle proteins of the yeast *Saccharomyces cerevisiae*. *J Bacteriol* 181, 6441-6448.

Froissard, M., Canonge, M., Pouteaux, M., Cintrat, B., Mohand-Oumoussa, S., Guillouet, S.E., Chardot, T., Jacques, N., and Casaregola, S. (2015) Lipids containing medium-chain fatty acids are specific to post-whole genome duplication *Saccharomycotina* yeasts. *BMC Evol Biol* 15, 97.

Kajiwara, K., Ikeda, A., Aguilera-Romero, A., Castillon, G.A., Kagiwada, S., Hanada, K., Riezman, H., Muñiz, M., and Funato, K. (2014). Osh proteins regulate COPII-mediated vesicular transport of ceramide from the endoplasmic reticulum in budding yeast. *J Cell Sci* 127, 376-387.

Kajiwara, K., Muneoka, T., Watanabe, Y., Karashima, T., Kitagaki, H., Funato, K. (2012). Perturbation of sphingolipid metabolism induces endoplasmic reticulum stress-mediated mitochondrial apoptosis in budding yeast. *Mol Microbiol* 86, 1246-1261.

Kajiwara, K., Watanabe, R., Pichler, H., Ihara, K., Murakami, S., Riezman, H., and Funato, K. (2008). Yeast ARV1 is required for efficient delivery of an early GPI intermediate to the first mannosyltransferase during GPI assembly and controls lipid flow from the endoplasmic reticulum. *Mol Biol Cell* 19, 2069-2082.

Kurokawa, K., Okamoto, M., and Nakano, A. (2014). Contact of cis-Golgi with ER exit sites executes cargo capture and delivery from the ER. *Nat Commun* 5, 3653.

Matsuura-Tokita, K., Takeuchi, M, Ichihara, A., Mikuriya, K., and Nakano, A. (2006). Live imaging of yeast Golgi cisternal maturation. *Nature* 441, 1007-1010.

Mumberg, D., Müller, R., and Funk, M. (1995). Yeast vectors for the controlled expression of heterologous proteins in different genetic backgrounds. *Gene* 156, 119-122.

Voynova, N.S., Vionnet, C., Ejsing, C.S., and Conzelmann, A. (2012). A novel pathway of ceramide metabolism in Saccharomyces cerevisiae. *Biochem J* 447, 103-114.